Journal of Applied Sciences

ISSN 1812-5654

science alert

ANSInet
an open access publisher
http://ansinet.com

Journal of Applied Sciences 14 (22): 3101-3105, 2014
ISSN 1812-5654 / DOI: 10.3923/jas.2014.3101.3105
© 2014 Asian Network for Scientific Information

Temperature Distribution of Single Slope Solar Still by Finite Difference Method

Kiam Beng Yeo, Kenneth Tze Kin Teo and Cheah Meng Ong
Materials and Minerals Research Unit, Faculty of Engineering, Universiti Malaysia Sabah,
Jalan UMS, Kota Kinabalu, 88400, Sabah, Malaysia

Abstract: Single slope solar still utilizes solar distillation technology to clean water from brackish water was investigated. The clean water output of solar still depends on the intensity of sunlight and how well the different mediums in solar still transfer the heat energy around. Thus, the temperature distribution in the single slope solar still was analysed using the explicit finite difference method. Side view of solar still is aligned with a mesh system, which accommodates nodes and specific equation to calculate the temperature at the next time-step for every derived node. Simulation result showed the trend of heat transfer process developing from the basin of solar still to the glass cover and the temperature recorded was about 65°C during 4 h of simulation time.

Key words: Finite difference method, single slope solar still, temperature distribution

INTRODUCTION

The clean water supply on earth is facing major challenges with the growing population. There is only about 0.3% of fresh water being accounted from the lakes and rivers among the 2.5% fresh water from the total amount of water on Earth (Kabeel, 2009; Ali *et al*., 2011). Although, there are many applicable water treatment methods at present but most of them operate at large capacities in cities and consume a lot of energy (Dev *et al*., 2011; Gude *et al*., 2011). On the contrary, single slope solar still applied solar distillation principle, which is natural hydrological cycle, to produce clean water from brackish and underground water at low cost (Alvarado-Juarez *et al*., 2013).

Over time, the operating behaviour of single slope solar stills have been modelled by researchers to evaluate its performance for different metrological, operational and design parameters (Ray and Jain, 2011). Compared to analytical solutions, numerical solutions such as Finite Difference Method (FDM) are more suitable to describe the heat transfer behaviour in the solar still. Unlike analytical solution, which only solves the average temperature of solar still, the finite difference method could predict the temperature readings at all the nodes within the grid system assigned. In solving heat transfer problems, authors such as Hsu (2006) and Yang *et al*. (2002) have shown excellent results in 2-D and 3-D heat conduction analysis.

In this study, the governing equations for different types of nodes in the 2-D grid system of a single slope solar still was derived. Heat transfer processes occurs around the nodes such as conduction, convection, insulation and heat generation are considered as well. With the knowledge of the surrounding behaviour, the governing equations can therefore be simulated and predicted.

GOVERNING EQUATION

In heat transfer analysis, FDM comes with a mesh, which is a set of locations where each point is referred as node distinguished by the local distance and time step between adjacent points. Generally, FDM can be classified into three types of scheme, which are explicit, implicit and Crank-Nicolson scheme. Explicit scheme uses forward difference in time to represent the rate of change of a node while the implicit scheme uses backward difference in time instead and Crank-Nicolson scheme with central difference in time.

Explicit scheme is chosen in this study due to easier implementation and least numerical intensive as compared to the other schemes, despite the concern about accuracy. For single slope solar still, a mesh consists of the nodes according to the side view of single slope solar still is shown in Fig. 1. The solar irradiance will first reach the basin through the glass cover with the assumption that all the outer walls of basin being insulated. The heat will

Corresponding Author: Kiam Beng Yeo, Materials and Minerals Research Unit, Faculty of Engineering, Universiti Malaysia Sabah, Jalan UMS, Kota Kinabalu, 88400, Sabah, Malaysia

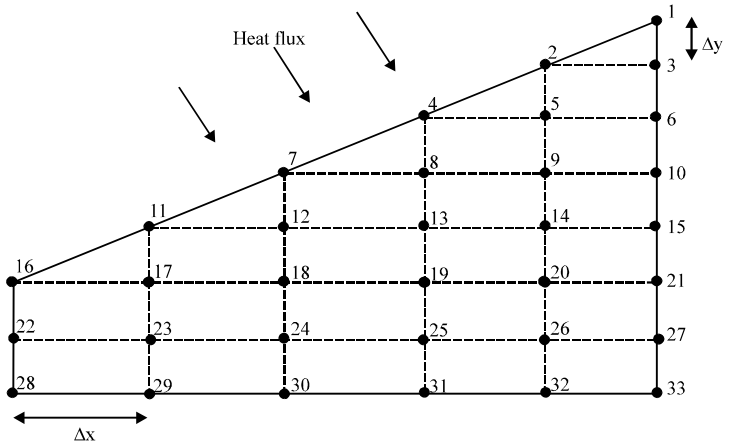

Fig. 1: Mesh and nodes positioning for single slope solar still (side view)

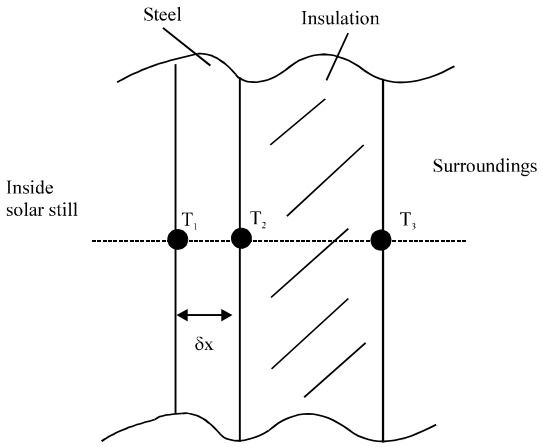

Fig. 2: Cross-sectional side view of the sides of solar still

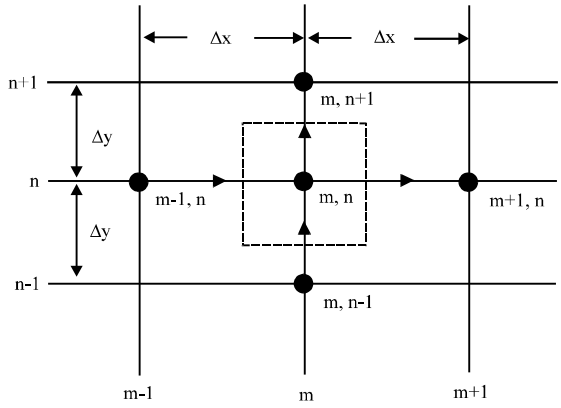

Fig. 3: Interior node with surrounding nodes

transfer from the basin to the water, eventually to the inside of solar still and glass cover then finally to the surroundings.

Before the computation of governing equation for the nodes, presumptions are made at the cross sectional side view of the solar still. From Fig. 2, there is a layer of insulation between the sides of solar still and the surroundings. In normal circumstances, there are heat conduction process in which heat transfer from T_1 to T_2, to T_3 then finally escape to the surroundings by convection process, which result in additional detailed computation specifically for this thin layer. However, with the assumptions that the solar still is perfectly insulated and the thickness of the steel, δx is very thin compared to x and y-axis interval (Δx and Δy) the minimum heat transfer activity of the highly non-thermal conductive insulation could be neglected and therefore, it reduces the governing equations into simpler FDM model.

The basic principle of FDM can be understood as the sum of rate of heat transfer at the surrounding nodes and rate of heat generation inside the node equals to the rate of change of energy content of the node. For interior nodes which are located within water or air medium, convection process take place. However, the direction of energy flowing in and out from these nodes may differ depending on the positioning of the nodes. Figure 3 shows the positioning of node 23 and the expression for the temperature at time p+1 is shown in the Eq. 1 and 2:

$$Q_{conv(m-1,\,n)\rightarrow(m,\,n)} + Q_{conv(m,\,n-1)\rightarrow(m,\,n)} = Q_{conv(m,\,n)\rightarrow(m,\,n+1)} + Q_{conv(m,\,n)\rightarrow(m+1,\,n)} + \frac{\Delta E_{m,\,n}}{\Delta t} \quad (1)$$

$$T_{m,\,n}^{p+1} = \left[1 - \left(\frac{2h\Delta t}{\rho c \Delta x}\right)\left(\frac{1}{\Delta x} + \frac{1}{\Delta y}\right)\right] T_{m,\,n}^{p} + \frac{h\Delta t}{\rho c \Delta y}\left(T_{m,\,n+1}^{p} + T_{m,\,n-1}^{p}\right) + \frac{h\Delta t}{\rho c \Delta x}\left(T_{m+1,\,n}^{p} + T_{m-1,\,n}^{p}\right) \quad (2)$$

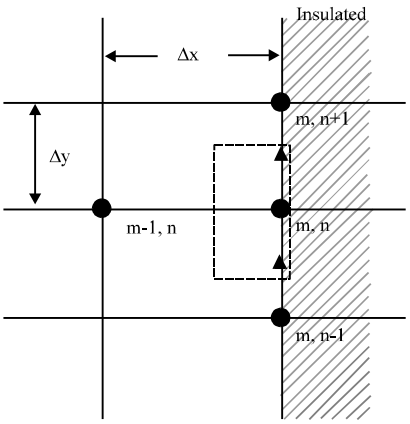

Fig. 4: Node distribution with one side insulation

For nodes with one-side insulated (Fig. 4), which are located on the sides of solar still, there are only three neighboring nodes left and no heat is allowed to escape to the insulated side. Heat is conducted for nodes in the same steel medium whereas convection process happened to the water or air medium inside the solar still. Equation 3 and 4 showed the expression for the temperature at time p+1 type of node:

$$Q_{cond(m,\,n-1)\to(m,\,n)} = Q_{conv(m,\,n)\to(m-1,\,n)} + Q_{cond(m,\,n)\to(m,\,n+1)} + \frac{\Delta E_{m,\,n}}{\Delta t} \quad (3)$$

$$T_{m,\,n}^{p+1} = \left[1 - \frac{2h\Delta t}{\rho c\Delta x} - \frac{2k\Delta t}{\rho c\Delta y^2}\right] T_{m,\,n}^{p} + \frac{2h\Delta t}{\rho c\Delta x} T_{m-1,\,n}^{p} + \frac{k\Delta t}{\rho c\Delta y^2}\left(T_{m,\,n+1}^{p} + T_{m,\,n-1}^{p}\right) \quad (4)$$

Besides that, for the nodes located at the bottom corner of solar still, node 28 and 33 experiences conduction heat transfer from two neighboring nodes and also received the heat energy from sunlight, whereas the top corner nodes, node 1 and 16 experiences both conduction and convection across different mediums. Equation 5 expresses the temperature for the two bottom corner nodes while Eq. 6 and 7 are specifically for node 1 and 16:

$$T_{m,\,n}^{p+1} = \left[1 - \left(\frac{2k\Delta t}{\rho c}\right)\left(\frac{1}{\Delta y^2} + \frac{1}{\Delta x^2}\right)\right] T_{m,\,n}^{p} + \left(\frac{2k\Delta t}{\rho c}\right)\left(\frac{T_{m,\,n+1}^{p}}{\Delta y^2} + \frac{T_{m+1,\,n}^{p}}{\Delta x^2}\right) + \frac{\Delta t}{\rho c}\dot{q} \quad (5)$$

$$T_{m,\,n}^{p+1} = \left[1 - \left(\frac{2k_g\Delta t}{\rho c}\right)\left(\frac{1}{\Delta x^2} + \frac{1}{\Delta y^2}\right) - \frac{k_s\Delta t}{\rho c\Delta y^2} - \left(\frac{4h_a\Delta t}{\rho c}\right)\left(\frac{1}{\Delta y} + \frac{1}{\Delta x}\right)\right] T_{m,\,n}^{p} + \left(\frac{2k_g\Delta t}{\rho c}\right)\left(\frac{1}{\Delta x^2} + \frac{1}{\Delta y^2}\right) T_{m-1,\,n-1}^{p} + \frac{k_s\Delta t}{\rho c\Delta y^2} T_{m,\,n-1}^{p} + \left(\frac{4h_a\Delta t}{\rho c}\right)\left(\frac{1}{\Delta y} + \frac{1}{\Delta x}\right) T_a \quad (6)$$

$$T_{m,\,n}^{p+1} = \left[1 - \left(\frac{2k_g\Delta t}{\rho c}\right)\left(\frac{1}{\Delta y^2} + \frac{1}{3\Delta x^2}\right) - \left(\frac{2h_w\Delta t}{\rho c\Delta x}\right) - \left(\frac{2h_a\Delta t}{\rho c}\right)\left(\frac{1}{\Delta y} + \frac{1}{\Delta x}\right)\right] T_{m,\,n}^{p} + \left(\frac{4k_g\Delta t}{3\rho c\Delta y^2}\right)\left(\frac{T_{m+1,\,n+1}^{p}}{2} + T_{m,\,n-1}^{p}\right) + \left(\frac{2k_g\Delta t}{3\rho c\Delta x^2}\right) T_{m+1,\,n+1}^{p} + \left(\frac{2h_w\Delta t}{\rho c\Delta x}\right) T_{m+1,\,n}^{p} + \left(\frac{2h_a\Delta t}{\rho c}\right)\left(\frac{1}{\Delta y} + \frac{1}{\Delta x}\right) T_a \quad (7)$$

Finally, for other nodes along the slope, which experience conduction process from the two diagonal neighbor nodes and also convection process from two adjacent nodes acted on the node, then Eq. 8 express the temperature of these nodes:

$$T_{m,\,n}^{p+1} = \left[1 - \left(\frac{k_g\Delta t}{2\rho c}\right)\left(\frac{1}{\Delta y^2} + \frac{1}{\Delta x^2}\right) - \left(\frac{h_a\Delta t}{\rho c}\right)\left(\frac{1}{\Delta x} + \frac{1}{\Delta y}\right) - \left(\frac{3h_a\Delta t}{4\rho c}\right)\left(\frac{1}{\Delta y} + \frac{1}{\Delta x}\right)\right] T_{m,\,n}^{p} + \left(\frac{k_g\Delta t}{2\rho c}\right)\left(\frac{1}{\Delta y^2} + \frac{1}{\Delta x^2}\right)\left(T_{m+1,\,n+1}^{p} + T_{m-1,\,n-1}^{p}\right) + \left(\frac{h_a\Delta t}{\rho c}\right)\left(\frac{1}{\Delta x} + \frac{1}{\Delta y}\right) T_a + \left(\frac{3h_a\Delta t}{4\rho c}\right)\left(\frac{T_{m,\,n-1}^{p}}{\Delta y} + \frac{T_{m+1,\,n}^{p}}{\Delta x}\right) \quad (8)$$

SIMULATION RESULT

The equations representing all the nodes of the single slope solar still mentioned above are simulated using MATLAB© software, with all the simulation parameters as stated in the Table 1. Figure 5 shows the temperature for all the nodes after 4 h of simulation time, the annual average solar irradiance readings implemented in the simulation is referred to the actual average solar irradiance readings recorded in a year at Kota Kinabalu, Sabah, Malaysia which is shown in Fig. 6. These solar irradiance readings were taken from 8 am to 6 pm. The peak of the solar irradiance reading occurred at the 4th h, which is approximately at 12 pm noon.

The water in the solar still has been assumed to fill up until the second row covering node 22 until node 33. The parameters of water as stated in the Table 1 have been utilized. Temperature readings of nodes at the bottom of the solar still has maintain a consistent value at approximately 65°C, due to the heat energy absorbed from sunlight and the no heat loss to the surroundings. The heat is then transferred to the glass cover and finally to the surroundings, which results in the decrement of temperature from node 33-1 at the sides of solar still. From the temperature readings in Fig. 5, the heat flow lines of single slope solar still can be deduced by observing the temperature difference of nodes in the same medium, which are glass, air, water and steel. The Fig. 7 illustrated the general heat flow lines of the solar still at minimum number of nodes and the x-axis and y-axis interval is coarse. A more complete and refine heat flow lines diagram can be achieved by increasing the number of nodes in the mesh.

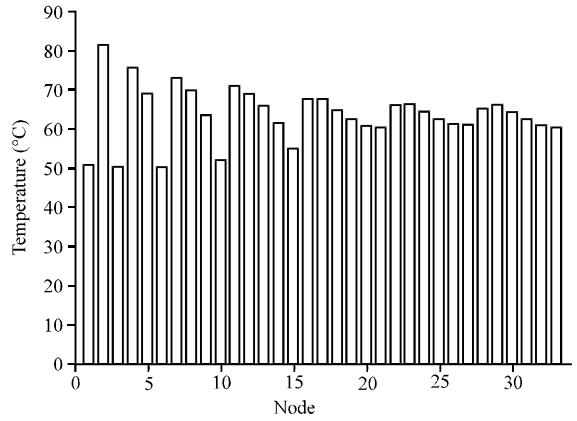

Fig. 5: Temperature of nodes during 4th h of simulation time

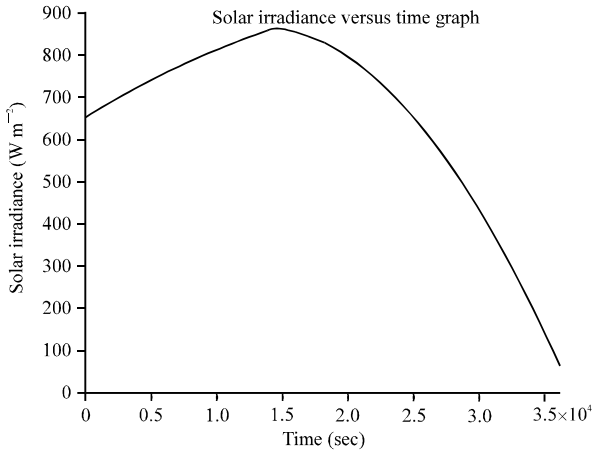

Fig. 6: Solar irradiance readings of a day in Kota Kinabalu, Sabah, Malaysia

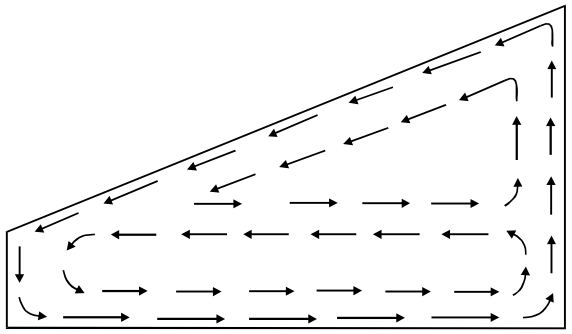

Fig. 7: Heat flow lines of single slope solar still

With no heat allowed to escape from the sides and bottom of solar still, the heat transfer process can only gradually transfer to the top, forming circulation due to the closed environment in the solar still. At the glass cover, heat is then escape to the surroundings by convection which allows water vapour to condensate into clean water. The water medium and air medium inside the solar still form its own heat transfer circulation, respectively. The heat flow of these two mediums is in the opposite direction, which allows the convection process between them.

Table 1: Parameters defined in the simulation

Parameters	Value
Glass cover density, ρ_g (kg m^{-3})	2500
Water density, ρ_w (kg m^{-3})	1000
Air density, ρ_a (kg m^{-3})	1.177
Steel density, ρ_s (kg m^{-3})	8000
Glass cover specific heat, c_g (J kg^{-1}. °C)	753
Water specific heat, c_w (J kg^{-1}. °C)	4187
Air specific heat, c_a (J kg^{-1}. °C)	1007
Steel specific heat, c_s (J kg^{-1}. °C)	400
Glass cover thermal conductivity, k_g (W m^{-1}. °C)	1.3
Water thermal conductivity, k_w (W m^{-1}. °C)	0.59
Air thermal conductivity, k_a (W m^{-1}. °C)	0.0263
Steel thermal conductivity, k_s (W m^{-1}. °C)	13.4
Water convective heat transfer coefficient, h_w (W m^{-2}. °C)	100
Air convective heat transfer coefficient, h_a (W m^{-2}. °C)	10
Initial temperature, T_0 (°C)	25
Horizontal distance between two nodes, Δx (m)	0.1
Vertical distance between two nodes, Δy (m)	0.058

CONCLUSION

The temperature distribution of single slope solar still is computed using the explicit finite difference method. Side view of solar still is aligned with a mesh system, which accommodates nodes and specific equations to calculate the temperature at the next time step for every node has been derived. Simulation result showed that the trend of heat transfer process is generated from the basin of solar still to the glass cover and the highest temperature recorded is about 65°C during 4 h of simulation time.

ACKNOWLEDGMENT

The authors are thankful to the Ministry of Higher Education Malaysia for funding this project (Grant No. FRG0310-TK-1/2012) and the Materials and Minerals Research Unit, School of Engineering and Information Technology, Universiti Malaysia Sabah for providing the support and facilities.

REFERENCES

Ali, M.I., R. Senthilkumar and R. Mahendren, 2011. Modelling of solar still using granular activated carbon in matlab. Bonfring Int. J. Power Syst. Integrated Circ., 1: 5-10.

Alvarado-Juarez, R., G. Alvarez, J. Xaman and I. Hernandez-Lopez, 2013. Numerical study of conjugate heat and mass transfer in a solar still device. Desalination, 325: 84-94.

Dev, R., H.N. Singh and G.N. Tiwari, 2011. Characteristic equation of double slope passive solar still. Desalination, 267: 261-266.

Gude, V.G., N. Nirmalakhandan and S. Deng, 2011. Desalination using solar energy: Towards sustainability. Energy, 36: 78-85.

Hsu, P.T., 2006. Estimating the boundary condition in a 3D inverse hyperbolic heat conduction problem. Applied Math. Comput., 177: 453-464.

Kabeel, A.E., 2009. Performance of solar still with a concave wick evaporation surface. Energy, 34: 1504-1509.

Ray, C. and R. Jain, 2011. Drinking Water Treatment: Focusing on Appropriate Technology and Sustainability. Springer Science and Business Media, New York, ISBN: 9789400711044, Pages: 280.

Yang, M.T., K.H. Park and P.K. Banerjee, 2002. 2D and 3D transient heat conduction analysis by BEM via particular integrals. Comput. Methods Applied Mech. Eng., 191: 1701-1722.